International Journal on Advanced Science Engineering Information Technology

Vol.13 (2023) No. 6
ISSN: 2088-5334

Analysis of Propagation Characteristics in Unmanned Aerial Vehicle (UAV) System

Eni Dwi Wardihani [a,*], Tiara Nira Sari [a], Thomas Agung Setyawan [a], Hany Windri Astuti [a]

[a] Department of Electrical Engineering, Politeknik Negeri Semarang, Jl. Prof. Soedarto, Tembalang, Semarang, Indonesia
Corresponding author: [*]edwardihani@polines.ac.id

***Abstract*—Unmanned Aerial Vehicle (UAV) has gained great attention to the spread of communication in civilian and military applications. UAV communication channel has its own characteristics compared to cellular and satellite systems, which are widely used. Thus, an accurate channel characterization is very important to optimize the performance and design of an efficient UAV communication system. However, several challenges exist in UAV channel modeling. For example, channel propagation characteristics of UAVs are still less explored. Therefore, this research discusses the propagation characteristics of UAV communication systems. Due to the limitation of the measurement tools, the propagation characteristics identified in this research was the pathloss coefficient value and optimum height based on the value of Received Signal Strength Indicator (RSSI) measurement results at different distance and heights. The link communication used 433 MHz telemetry. The results of pathloss coefficient at heights of 10 m, 20 m, and 30 m are 1.56 m, 1.77 m, and 1.99 m. While the results of the optimum height of 10 m, 20 m, and 30 m are 1.39 m, 1.32 m, and 1.47 m.**

***Keywords*—Hexacopter; optimum height; pathloss coefficient; propagation.**

Manuscript received 3 Sep. 2022; revised 7 Nov. 2022; accepted 7 Jan. 2023. Date of publication 31 Dec. 2023.

I. INTRODUCTION

Unmanned Aerial Vehicle (UAV) is a flying machine which can be controlled by a remote control or an aircraft without any aircraft crew controlling it. The development of UAVs could change architecture and operations through the characteristics and capabilities due to evolution [1]–[3]. UAV can carry cameras, sensors, communication devices, and several other pieces of equipment [4]. This kind of aircraft is widespread in the military and has many functions, one of which can be used to photograph, record, monitor, and cover an object from the air using a camera mounted on an aircraft. Unmanned aircraft are also increasingly being used for civilian purposes such as firefighting, non-military security, supervision of protected areas, and conducting searches to save victims [5]. A wireless communication line is needed to carry out that monitoring, which connects the UAV to the ground station with high data transfer speeds and a considerable distance [6]–[8].

Two variations of aircraft control are controlled by remote control or flying independently based on the program that has been entered using the Ground Control Station software. Ground Control Station (GCS) is software used on computers that are utilized by the UAV system to provide the input and receive the data from UAV hexacopter models via wireless telemetry devices. GCS software commonly used in the UAV system is Mission Planner, Ground Control, HappyKillMode GCS and so on. Some GCS can record the flight data obtained from sensors installed on the autopilot device. Flight routes or waypoints can also be determined in the GCS [9]–[11] to fly hexacopter autonomously.

Tracking waypoint motion planning has the task of giving UAV flight action from a free position to the next waypoint [9]–[11]. Eventually, this tracking waypoint is responsible for directing the UAV to a predetermined waypoint point following the optimal flight path between the waypoints [12]. The speed and distance of UAV can be adjusted in the waypoint planning. UAV flights are usually used for observation missions that are required to send data to the ground station. On the delivery, there are propagation losses in the form of attenuation by distance to the speed of the hexacopter. The network infrastructure uses the Received Signal Strength Indicator (RSSI) in its measurement method.

RSSI is a technology used for measuring the signal strength indicators received by a wireless device [13]–[15]. However, direct mapping of RSSI values based on distance has many limitations because RSSI is susceptible to noise, multi-path fading, interference, etc., which results in large fluctuations in the received power [16], [17].

II. Materials and Method

A. Propagation

Radio wave propagation can be categorized into two, namely propagation in space (indoor) and outdoor propagation (outdoor) [18]. All the basic radio propagation modeling is called the free space propagation model. Free space propagation is when the transmitter and receiver are not blocked by anything. Free space propagation serves to estimate the Gain from the signal at the receiver [19]. The basic mechanism of propagation is shown in Fig.1, which describes the occurrence of reflection, diffraction, and scattering [20].

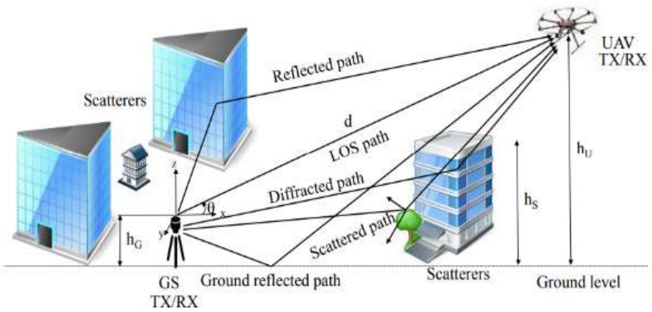

Fig. 1 Radio wave propagation mechanism.

Pathloss communication from Air to Ground is calculated using propagation modeling. This propagation model is a modification of the free space pathloss formula by using distance and height to measure propagation in UAV. There are two variations of propagation modeling, namely dynamic UAV and static UAV. The propagation modeling formula for static UAV [21], [22] is as Eq. (1).

$$PL(d)=PLo+10n\log10(\frac{d}{d0})-10\log10(\frac{\Delta h}{hopt})+10\log10cp+S \quad (1)$$

Where PLo is the pathloss reference from the reference of distance; n is the pathloss exponent value; Δh got from $|hgnd - hopt|$, $hgnd$, is the height of receiver on the ground, while *hopt* is the minimum height of receiver which can give a small pathloss;*Cp* got from *10 log10 Cp>0 dB*, is constant loss factors due to foliage and losses due to antenna orientation on the UAV and S is Shadowing variable. The propagation modeling formula for dynamic UAV [23], [24] is shown in Eq. (2).

$$PL(d)=PLo+10nlog_{10}(\frac{d}{d0})-10log_{10}(\frac{\Delta h}{hopt})+10log_{10}c_p+10x\,log10(\frac{(fe+\Delta f)}{fe})+S \quad (2)$$

Δf is got from $\left(\frac{\Delta v}{c}\right)*fe$, it is Doppler variation in frequency at relative speed (v) of UAV to the receiver on the ground; fe is the transmitted frequency, while f got from $fe+\Delta f$, is the observed frequency at the receiver and x is the pathloss factor frequency. At the speed of less than 10 m / s, a factor of $10x$ log10 $((fe+\Delta f)/fe)$ is negligible.

B. Received Signal Strength Indicator (RSSI)

The Received Signal Strength Indicator (RSSI) measures the received radio signal power amount in telecommunications. A user from the receiving device can see RSSI. Due to the unit of RSSI in the Mission Planner software point, it is converted into RSSI dBm signal [25] with the following formula in Eq. (3).

$$signal\_dBm = (RSSI / 1.9) - 127 \quad (3)$$

C. Linear Regression

Simple linear regression is based on one independent variable's functional relationship or causal with one dependent variable. The general equation of simple linear regression is seen in Eq. (4) and (5) [26] :

$$Y = a + bX$$

$$a = \frac{(\sum Y1)(\sum X1^2)-(\sum X1)(\sum X1\,Y1)}{n\sum X1^2-(\sum X1^2)} \quad (4)$$

$$b = \frac{n\sum X1\,Y1-(\sum X1)(\sum Y1)}{n\sum X1^2-(\sum X1^2)} \quad (5)$$

Y is the predicted dependent variable, *X* is the independent variable with a certain value, while *a* is a constant, and *b* is the regression coefficient *X* to *Y*. In this research, the testing was done by the state without any obstacle (Line of Sight), and the hexacopter used a maximum speed of 5m/s. Then according to Eq. (2), the Doppler effect, factor foliage loss, and shadowing can be ignored. The linear regression equation in this research is indicated an equation with propagation modeling such as Eq. (6).

$$PL = PL\,(d0) - 10\,log\,\frac{\Delta h}{hopt} + 10\,n\,(log_{10}\,\frac{d}{d0}) \quad (6)$$

The variable Y is PL, and the variable a is $PL\,(d0) - 10\,log\,\frac{\Delta h}{hopt}$ and the variable bX is $10\,n\,(log_{10}\,\frac{d}{d0})$. In Eq. (6) above, Δh is equal to $|h_{gnd} - h_{opt}|$, h_{gnd} is the height of the receiver on the ground, h_{opt} is the minimum height which can give a small value of RSSI, equation a is as a reference distance pathloss subtracted by the height while b is *10n* and X is logarithmic distance to the reference distance of $log\frac{d}{d0}$. Thus, finding pathloss exponent is done by using the formula of *b/10*. After searching for the pathloss exponent, then seek the optimum height of the equation a. This is how to seek for *hopt* using Eq. (7).

$$Hopt = \frac{hgnd}{10^{\frac{PL\,(d0)-a}{10}}+1} \quad (7)$$

Fig. 2 is an overview of the parameters used for finding the pathloss coefficient value as well as optimum height.

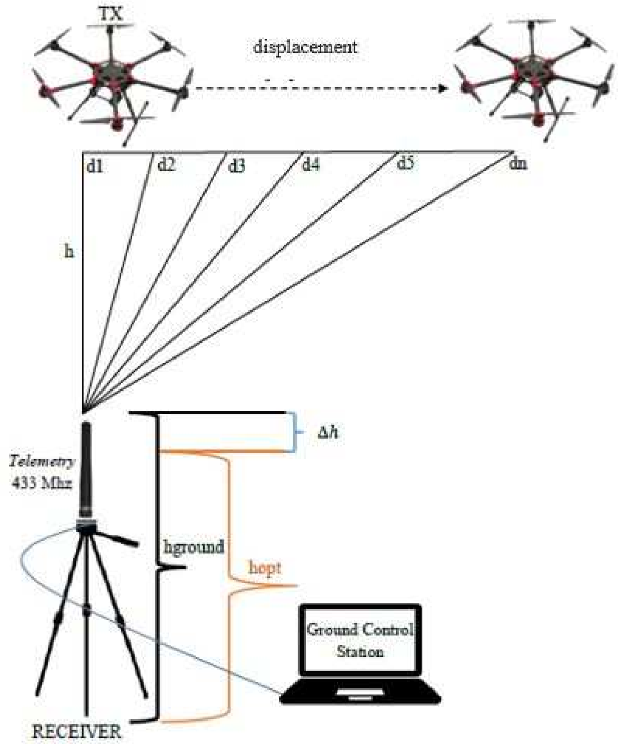

Fig. 2 The parameter used in this research

D. System Design

The flight controller PIXHAWK was used as a main board for hexacopter controller. Hexacopter has two communication links between sky surfer with radio control at 2.4 GHz and telemetry data at 433 MHz. This system is shown below in Fig. 3.

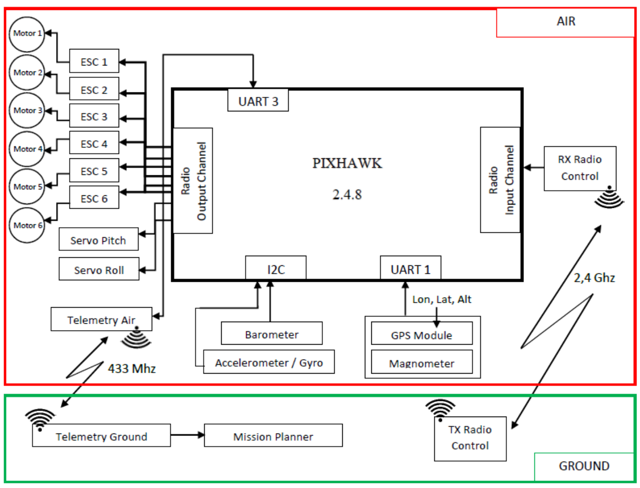

Fig. 3 Diagram block of the entire system design

Radio control gives orders to the hexacopter analogously, while the telemetry functions provide the appropriate waypoint commands for autopilot drawn on the Mission Planner via serial USB. In Fig. 4, as we were going to fly the hexacopter, we had to connect the telemetries in advance so that the air and ground telemetry could communicate. By those telemetries, the hexacopter will fly according to the waypoint mission. From the waypoint, 433 MHz will transmit the telemetry data such as height, distance, and RSSI shown on the Ground Control Station. The telemetry's RSSI value will vary according to the distance and height changes.

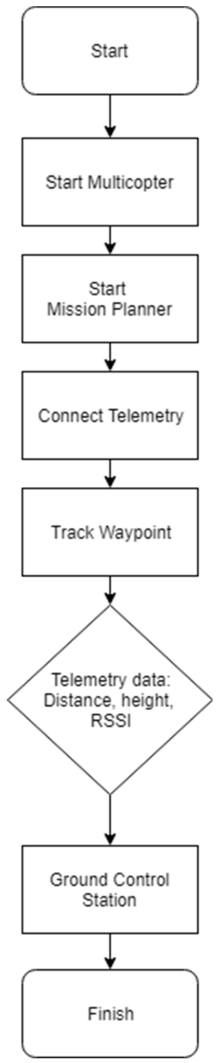

Fig. 4 System flowchart

The focus of this research was to analyze the results of Received Signal Strength Indicator (RSSI), which were received by the ground telemetry module on the different height and distances of the flight. The result of RSSI and the hexacopter distance of flight were processed through a linear regression indicating a propagation modeling to determine the coefficient of pathloss and the optimum height of the environment.

E. Testing Scenario

Flight planning is designed to facilitate the orientation in data retrieval [27]. The flight planning was made using the software Mission Planner 3.1.56. The testing scenario would be carried out in a vacant lot near Villa Mulawarman, Semarang, Indonesia, because the area is flat and wide. There are no distractions, such as large buildings and trees, so it is feasible to take the data in the Line of Sight way. The waypoint was made at 10, 20, 30, and 40 m with a flight range of 80 m and a constant speed of 5 m /s.

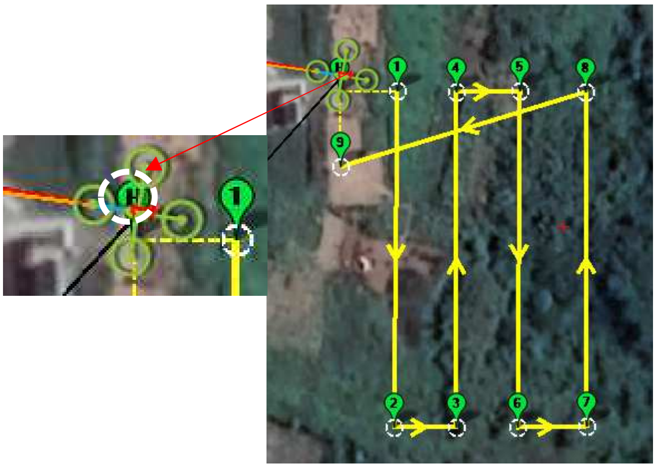

Fig. 5 Flight planning on Mission Planner (right) dan Home as a Ground Control Point (left)

The Home in Fig. 5, as shown with the letter "H" in the dashed white line, serves as the Ground Control Station (GCS). The data collection was performed by observing changes in the Received Signal Strength Indicator (RSSI) value based on distance and height depending on the Telemetry Logs. Fig. 6 is an overview of the testing scenario in this research.

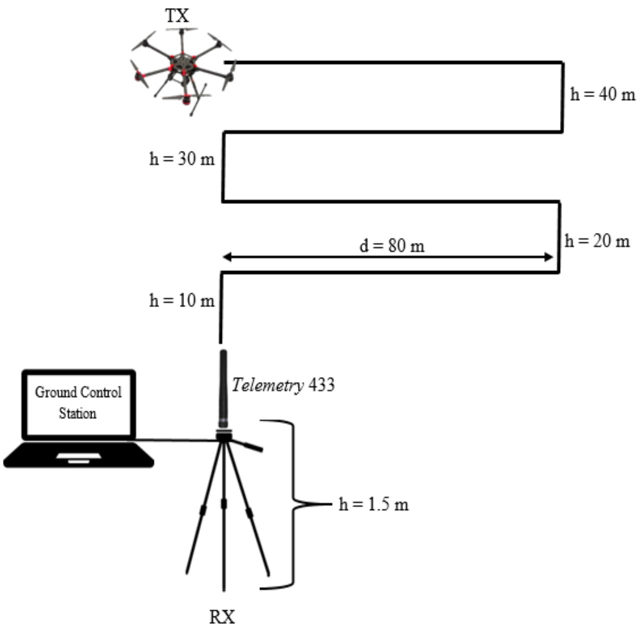

Fig. 6 Testing scenario

III. Results and Discussion

A. Result of Working System Testing

The test result includes the result of the radiation pattern in the telemetry antenna 433 MHz, the average signal strength (Value A), and the working distance test result. Telemetry antenna 433 MHz is omnidirectional shaped. After obtaining the data, the next step is calculating the average RSSI at each corner and making a chart in Excel. Thus, it obtained the telemetry antenna radiation pattern 433 MHz shown in Fig. 7.

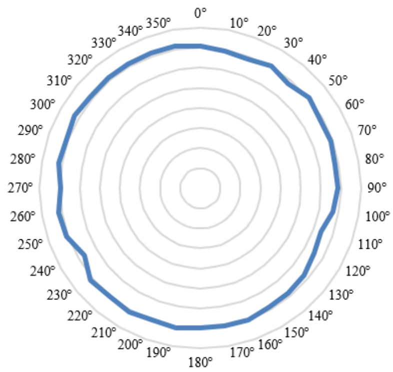

Fig. 7 Telemetry antenna radiation pattern 433 MHz

The radiation pattern of the test results obtained the average signal strength (Value A). Fig. 8 shows the graph of RSSI (Received Signal Strength Indicator) values in each corner and the results of the average value in -55.61 dBm signal strength. RSSI indicates the signal level reception. This value determines whether the signal received is sufficient or not to access the wireless network. Regarding the level of RSSI, the value of -55.61 dBm is categorized very good signal [28].

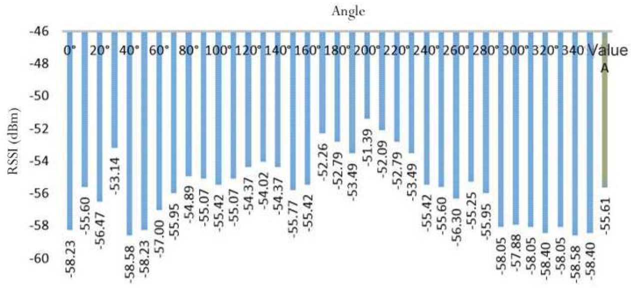

Fig. 8 Graph of average signal strength

The testing result of the working distance telemetry antenna 433 MHz on the ground test was 116.81 m with RSSI 57 (-97 dBm). In Fig. 9, it can be seen in the red box the signal reception that has been crossed, meaning that it is unable to receive the signal anymore.

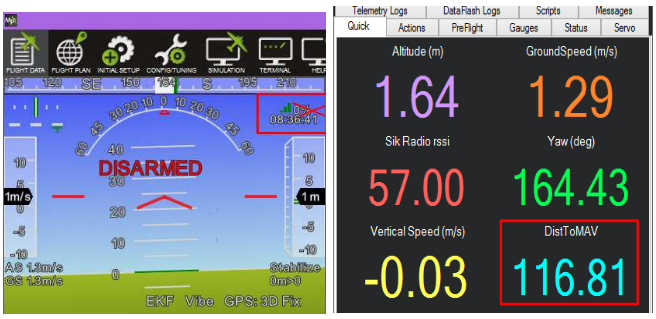

Fig. 9 The testing result of the working distance of UAV orientation (in left) and UAV parameter (in right)

B. Results of Data Collection

The data collection according to flight planning and scenario testing are outlined in point E. Testing Scenario. At the waypoint that has been drawn on a Mission Planner, Fig. 10 shows the results of the hexacopter flight path that has flown on the vacant lot in Villa Mulawarman. The UAV flew from the take-off point, shown by the red color. The circles in green show the UAV position. The UAV took off and landed in the same place. The UAV runs autonomously following the flight path. It is possible for the telemetry functions to command the autopilot according to the flight path drawn in Mission Planner.

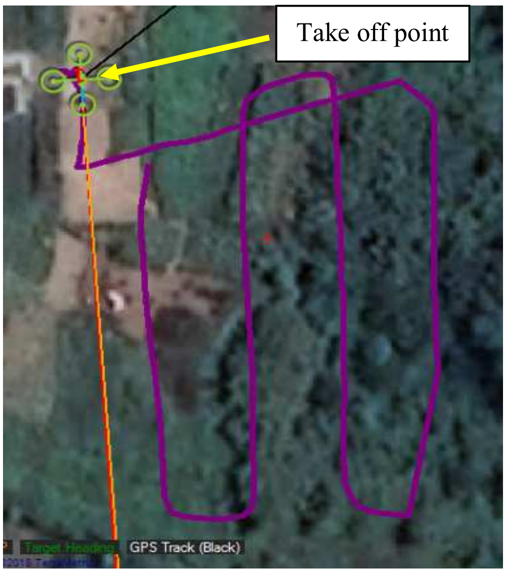

Fig. 10 Flight path of the hexacopter

C. Results and Analysis at Height 10 m

From the test result at the height of 10 m, the data required was the RSSI as *[Y]* and logarithmic distance to the reference distance $log \frac{d}{d0}$ *as [X]*. Then, the value of *X* and *Y* were incorporated into the linear regression that was created. It eventually displayed the result of the equation $Y = a + bx$. From the value of *a*, we could find the optimum height *(hopt)* and the value of *b*, we could find the value of *n* (coefficient pathloss). The linear regression equation indicated the propagation modeling used in this research, which can be seen in Eq. (6).

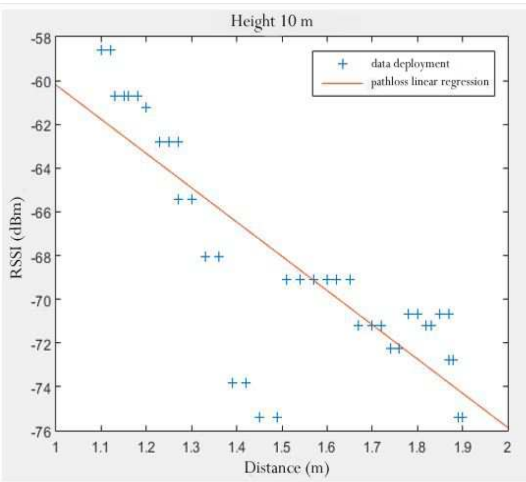

Fig. 11 Linear regression graph at a height of 10 m

Fig.11 is the result of the linear regression graph computation, and it obtained Y = [-45.5462] + [15.6576] x. According to Eq. (6), the value of n (coefficient pathloss) is b / 10. Thus, the value of n (coefficient pathloss) at a height of 10 m is 1.57. After finding the value of n (coefficient pathloss), find the optimum height value from equation a. To find the value of a, we can use Eq. (7). The value of PL (d0) has been obtained from the testing of the average signal strength that is -55.61 dBm and the antenna height from the ground laying (hgnd) of 1.5. In comparison, the result of hopt is 1.3911 m.

D. Testing Result and Analysis at Height 20 m

The linear regression equation indicated to the modeling of propagation used in this research can be seen in Eq. (6). Fig. 12. is the result of a linear regression graph at a height of 20 m. The graph obtained the equation of *Y = [-46.8837] + [17.7101] X.*

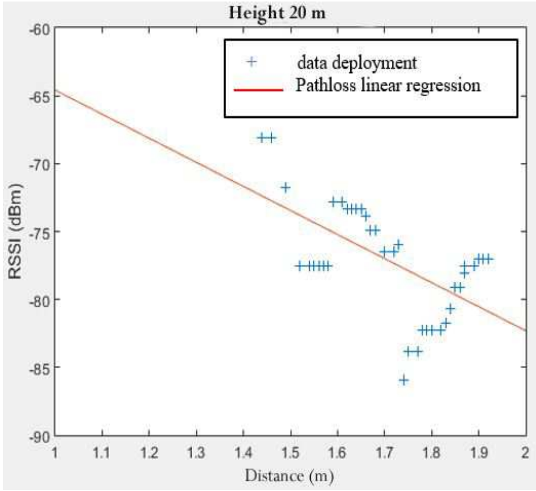

Fig. 12 Linear regression graph at a height of 20 m

According to the Eq. (6), *n* values (coefficient pathloss) is *b / 10* then the value of *n* (coefficient pathloss) at a height of 20 m is 1.77. The *PL (d0)* result is -55.61, and *the hgnd* is 1.5 m. The equation was entered to find the optimum height value, and the result of the computation obtained optimum height (hopt) value of 1.3227 m.

E. Testing Result and Analysis at Height 30 m

The linear regression equation that indicates the propagation modeling used in this research can be seen in Eq. (6). Fig. 13 is the result of a linear regression graph at a height of 30 m. The graph obtained equation *Y = [-38.3799] + [19.9757] X.*

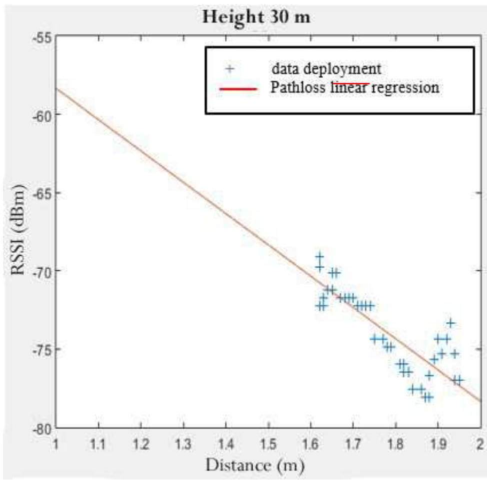

Fig. 13 Linear regression graph at a height 30 m

So, according to the Eq. (6), *n* value (coefficient pathloss) is *b / 10* then the value of *n* (coefficient pathloss) at a height of 30 m is 1.99. The result of *PL (do)* is -55.61 the *hgnd* is 1.5 m. The calculation of finding the optimum height values was done by entering the equations and the result of the computation obtained *hopt* = 1.4721 m.

TABLE I
CALCULATION RESULT OF PATHLOSS COEFFICIENT AND OPTIMUM HEIGHT

Height	Linear Regression Equation	Pathloss Coefficient *(n)*	Optimum Height *(hopt)*
10 m	*Y = [-44.5462] + [15.6576]x*	1.56	1.3911 m
20 m	*Y = [-46.8837] + [17.7101]x*	1.77	1.3227 m
30 m	*Y = [-38.3799] + [19.9757]x*	1.99	1.4721 m

Table 1 shows that the coefficient of pathloss increases along with the increasing height. Pathloss coefficient strongly influences the quality decrease of a communication link [29]–[31]. The contours of the terrain and environmental condition also influence pathloss coefficient. In terms of data collection in this research is done on the condition of Line of Sight or no obstacles at all, the pathloss coefficient value obtained is not too large. Optimum height is the minimum height to put the receiver antenna on the ground. Fig. 14 shows that the result is less than 1.5 m and the RSSI value of the testing result is 121 (-63.32 dBm).

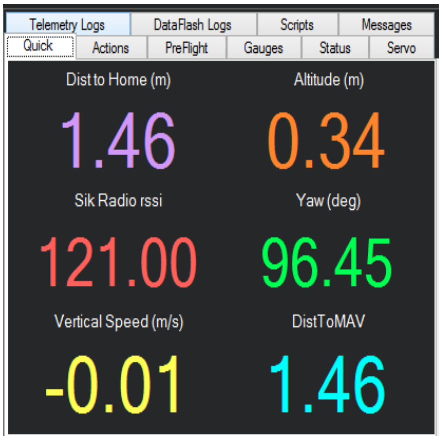

Fig. 14 RSSI results by distance <1.5 m

The value of RSSI either in 10 m, 20m or 30 m resulted in -55.61 dBm. This value is categorized as very good. So that the signal reception can run well enough to get a good wireless connection. Radio link can be considered good when the RSSI is >-115 dB., because the closer to 0 dBm, the better the signal is. Meanwhile, the value of pathloss coefficient is closer to the category of in building line of sight, as it is in the range of 1.6 – 1.8 [32]. Line of Sight (LoS) is the imagery line between the observer and the target. This condition creates a direct path of communication from a transmitter to the receiver. The Line of Sight condition is important in wireless network to create a high-speed communication [33].

Unmanned Aerial Vehicle (UAV) has been through a very long history in technological development as the invention of airplane. The increasingly popular UAV is important in terrain mapping, environment data collection, border monitoring, fire monitoring, etc. UAV can fly a few meters from the ground and acquire aerial data. However, it relies on the weather conditions. The UAV can have an unstable operation when the weather is not supportive. Related to the communication link in UAV, the effect of the environment, such as fading, can lead to signal degradation and influence the performance of the UAV itself. Especially in urban areas, vegetation has a significant impact because there are many scatters [34], [35].

One important thing in UAV is radio propagation used in the network. The shadowing model can generate simulation results which is different from free space loss and two-ray ground models. The free space propagation model assumes the transmitter and the receiver is in space without obstacle. Meanwhile, the two-ray ground propagation model assumes two signal paths from the transmitter to the receiver. The shadowing model shows lower performance than those models in case of its throughput, packet loss rate and packet delays [36]. Therefore, determining the radio propagation model in UAV network is important as it relates to the results.

IV. CONCLUSION

Based on the observation, pathloss coefficient values (n) and the optimum height (hopt) at the height of 10 m are 1.56 and 1.39 m, while at the height of 20 m are 1.77 and 1.32 m and at the height of 30 m are 1.99 and 1.47 m. Pathloss coefficient has a very strong effect on the quality of a communication link and is affected by the terrain's contours and environmental conditions. RSSI is very varied along the flight because the signal is attenuated when hexacopter is rolling (rolled over). The farthest distance that a 433 MHz telemetry can cover is 116.81 m. The average value of telemetry signal strength at 433 MHz is -55.61 dBm. The telemetry communication signal 433 MHz will decrease the distance and flying height of UAV.

ACKNOWLEDGMENT

We thank Politeknik Negeri Semarang and the director for the support and facilities, such as the laboratory and the equipment, which assisted the research.

REFERENCES

[1] F. Ahmed, J. C. Mohanta, A. Keshari, and P. S. Yadav, "Recent Advances in Unmanned Aerial Vehicles: A Review," *Arab. J. Sci. Eng.*, vol. 47, no. 7, pp. 7963–7984, 2022, doi: 10.1007/s13369-022-06738-0.

[2] N. Delavarpour, C. Koparan, J. Nowatzki, S. Bajwa, and X. Sun, "A technical study on UAV characteristics for precision agriculture applications and associated practical challenges," *Remote Sens.*, vol. 13, no. 6, pp. 1–25, 2021, doi: 10.3390/rs13061204.

[3] Hildanus, S. D. Tarigan, K. Murtilaksono, and B. Barus, "Mapping Land Use and Land Cover in the Upper Ciliwung Watershed Using Landsat Tree Cover (TC) Data," *Int. J. Adv. Sci. Eng. Inf. Technol.*, vol. 11, no. 6, pp. 2247–2253, 2021, doi: 10.18517/ijaseit.11.6.15712.

[4] S. A. H. Mohsan, M. A. Khan, F. Noor, I. Ullah, and M. H. Alsharif, "Towards the Unmanned Aerial Vehicles (UAVs): A Comprehensive Review," *Drones*, vol. 6, no. 6, pp. 1–27, 2022, doi:10.3390/drones6060147.

[5] D. Lesmana, Y. Permana, B. Santoso, and A. Infantono, "Military Drone Applications by Using Indonesian Defense Equipment for Over the Horizon Operations," *Pros. Semin. Nas. Sains Teknol. dan Inov. Indones.*, vol. 3, no. November, pp. 1–10, 2021, doi:10.54706/senastindo.v3.2021.149.

[6] R. Masroor, M. Naeem, and W. Ejaz, "Resource management in UAV-assisted wireless networks: An optimization perspective," *Ad Hoc Networks*, vol. 121, no. June, p. 102596, 2021, doi:10.1016/j.adhoc.2021.102596.

[7] V. Papić, P. Šolić, A. Milan, S. Gotovac, and M. Polić, "High-resolution image transmission from uav to ground station for search and rescue missions planning," *Appl. Sci.*, vol. 11, no. 5, pp. 1–19, 2021, doi: 10.3390/app11052105.

[8] A. Achmad, I. S. Areni, E. Palantei, A. D. Achmad, and Muliadi, "IoT Network of Sensor Array for Intrusion Detection and Diagnosis of Electrical Systems," *Int. J. Adv. Sci. Eng. Inf. Technol.*, vol. 12, no. 2, pp. 446–452, 2022, doi: 10.18517/ijaseit.12.2.13656.

[9] Alfiandy, M. T. Suprayogi, Nurwulan F, and M. Pfis, "Iot (Internet of Things) Navigasi Drone Berdasarkan Waypoint Iot (Internet of Things) Navigation Drone Based on Waypoint," *e-Proceeding Eng.*, vol. 8, no. 2, pp. 1–8, 2021.

[10] M. Samy, K. Amer, M. Shaker, and M. ElHelw, "Drone Path-Following in GPS-Denied Environments using Convolutional Networks," *arXiv*, vol. abs/1905, no. 01658, pp. 1–7, 2019.

[11] D. Hanto *et al.*, "A Simple and Cost-Effective Physical Distancing Violation Detector Using a Rotating Time of Flight Lidar," *Int. J. Adv. Sci. Eng. Inf. Technol.*, vol. 12, no. 3, pp. 1073–1079, 2022.

[12] Y. LIU, X. ZHANG, Y. ZHANG, and X. GUAN, "Collision free 4D path planning for multiple UAVs based on spatial refined voting mechanism and PSO approach," *Chinese J. Aeronaut.*, vol. 32, no. 6, pp. 1504–1519, 2019, doi: 10.1016/j.cja.2019.03.026.

[13] B. Wei, H. Song, J. Katto, and T. Kikkawa, "RSSI-CSI Measurement and Variation Mitigation with Commodity WiFi Device," *arXiv*, vol. 2203, no. 12888, pp. 1–9, 2022.

[14] S. Li, S. Welsen, and V. Brusic, "Multi-AP and Test Point Accuracy of the Results in WiFi Indoor Localization," *Sensors*, vol. 22, no. 10, pp. 1–19, 2022, doi: 10.3390/s22103709.

[15] S. K. Sahoo and P. K. Behera, "Path Loss-A Parameter that Affects Channel Performance in Mobile Communication," *Natl. J. Comput. Sci. Technol.*, vol. 3, no. 2, pp. 34–36, 2020.

[16] S. Naghdi and K. O. Keefe, "Detecting and Correcting for Human Obstacles in BLE Trilateration Using Artificial Intelligence," *sensors*, vol. 20, no. 1350, pp. 1–17, 2020.

[17] S. Yucer *et al.*, "RSSI-based Outdoor Localization with Single Unmanned Aerial Vehicle," *ArXiv*, vol. abs/2004, no. 10083, pp. 1–6, 2020.

[18] A. A. Segun, F. I. Isaac, and À. George, "Effects of Building Materials and Structures on Indoor Path Loss of Very High Frequency Radio Wave," *Am. J. Eng. Res.*, vol. 11, no. 02, pp. 73–80, 2022.

[19] J. Isabona and A. L. Imoize, "Terrain-based adaption of propagation model loss parameters using non-linear square regression," *J. Eng. Appl. Sci.*, vol. 68, no. 1, pp. 1–19, 2021, doi: 10.1186/s44147-021-00035-7.

[20] J. Gomez-Rojas, B. Medina-Delgado, and W. Palacios-Alvarado, "Diffuse scattering and physical optics in the propagation of electromagnetic waves applied to mobile communications," *J. Phys. Conf. Ser.*, vol. 2102, no. 1, pp. 1–6, 2021, doi: 10.1088/1742-6596/2102/1/012009.

[21] W. Khawaja, I. Guvenc, and D. Matolak, "UWB Channel Sounding and Modeling for UAV Air-to-Ground Propagation Channels," in *IEEE Globecom Conference*, 2016, pp. 1–7.

[22] A. Kachroo *et al.*, "Unmanned Aerial Vehicle-to-Wearables (UAV2W) Indoor Radio Propagation Channel Measurements and Modeling," *IEEE Access*, vol. 7, pp. 73741–73750, 2019, doi: 10.1109/access.2019.2920103.

[23] W. Khawaja, O. Ozdemir, F. Erden, I. Guvenc, and D. W. Matolak, "Ultra-Wideband Air-to-Ground Propagation Channel Characterization in an Open Area," *IEEE Trans. Aerosp. Electron. Syst.*, vol. 56, no. 6, pp. 4533–4555, 2020, doi:10.1109/TAES.2020.3003104.

[24] A. U. Darajat, M. Komarudin, and S. R. S, "Sistem Telemetri Unmanned Aerial Vehicle (UAV) BERBASIS Inertial Measurement Unit (IMU)," *Electr. J. Rekayasa dan Tek. Elektro*, vol. 6, no. 3, pp. 169–177, 2012.

[25] J. Harley, "Advanced Con Guration Monitoring The Link Quality," *Sik Radio*, 2018. .

[26] A. Goldsmith, *Wireless Communications*. Cambridge university press, 2005.

[27] E. E. Papadopoulou, C. Vasilakos, N. Zouros, and N. Soulakellis, "DEM-based UAV flight planning for 3D mapping of geosites: The case of olympus tectonic window, Lesvos, Greece," *ISPRS Int. J. Geo-Information*, vol. 10, no. 8, pp. 1–19, 2021, doi: 10.3390/ijgi10080535.

[28] Metageek, "Acceptable Signal Stregths," 2020. https://www.metageek.com/training/resources/understanding-rssi.html (accessed Nov. 6, 2022).

[29] M. Ayad, R. Alkanhel, K. Saoudi, M. Benziane, S. Medjedoub, and S. S. M. Ghoneim, "Evaluation of Radio Communication Links of 4G Systems," *Sensors*, vol. 22, no. 10, p. 3923, 2022, doi:10.3390/s22103923.

[30] M. Pinem, M. Zulfin, I. V. Sari, and S. I. Rezkika, "Parameter Analysis of Semi Deterministic Pathloss against Soft Handover Performance in Mobile Communication," in *Proceedings of the International Conference of Science, Technology, Engineering, Environmental and Ramification Researches (ICOSTEERR 2018)*, 2020, no. Icosteerr 2018, pp. 243–247, doi: 10.5220/0010080502430247.

[31] R. Shrestha *et al.*, "The effect of angular dispersion on THz data transmission," *Sci. Rep.*, vol. 12, no. 10971, pp. 1–9, 2022, doi:10.1038/s41598-022-15191-w.

[32] V. O. A. Akpaida, F. I. Anyasi, S. I. Uzairue, and A. I. Idim, "Determination of an Outdoor Path Loss Model and Signal Penetration Level in Some Selected Modern Residential and Office Apartments in Ogbomosho, Oyo State, Nigeria," *J. Eng. Res. Reports*, pp. 1–25, 2018, doi: 10.9734/jerr/2018/v1i29804.

[33] J. H. Goh, A. Shaw, and A. I. Al-Shamma'A, "Line-of-Sight Underwater Wireless Communication System," *Sci. Res. J.*, vol. 178, no. Vii, pp. 12–30, 2020, doi: 10.1088/1742-6596/178/1/012029.

[34] W. Khawaja, I. Guvenc, D. W. Matolak, U. C. Fiebig, and N. Schneckenburger, "A Survey of Air-to-Ground Propagation Channel Modeling for Unmanned Aerial Vehicles," *IEEE Commun. Surv. Tutorials*, vol. 21, no. 3, pp. 2361–2391, 2019, doi:10.1109/COMST.2019.2915069.

[35] D. L. Leite, P. J. Alsina, M. M. d. M. Campos, V. A. de Sousa, and A. A. M. de Medeiros, "Unmanned aerial vehicle propagation channel over vegetation and lake areas: First-and second-order statistical analysis," *Sensors*, vol. 22, no. 1, pp. 1–18, 2022, doi:10.3390/s22010065.

[36] I. F. Kenmogne, V. Drevelle, and E. Marchand, "Using Constraint Propagation for Cooperative UAV Localization from Vision and Ranging," *Stud. Syst. Decis. Control*, vol. 276, pp. 133–138, 2020, doi:10.1007/978-3-030-40814-5_16.